NASA/TM—2002-211325

Mechanical Testing of IN718 Lattice Block Structures

David L. Krause and John D. Whittenberger
Glenn Research Center, Cleveland, Ohio

Pete T. Kantzos and Mohan G. Hebsur
Ohio Aerospace Institute, Brook Park, Ohio

January 2002

The NASA STI Program Office . . . in Profile

Since its founding, NASA has been dedicated to the advancement of aeronautics and space science. The NASA Scientific and Technical Information (STI) Program Office plays a key part in helping NASA maintain this important role.

The NASA STI Program Office is operated by Langley Research Center, the Lead Center for NASA's scientific and technical information. The NASA STI Program Office provides access to the NASA STI Database, the largest collection of aeronautical and space science STI in the world. The Program Office is also NASA's institutional mechanism for disseminating the results of its research and development activities. These results are published by NASA in the NASA STI Report Series, which includes the following report types:

- TECHNICAL PUBLICATION. Reports of completed research or a major significant phase of research that present the results of NASA programs and include extensive data or theoretical analysis. Includes compilations of significant scientific and technical data and information deemed to be of continuing reference value. NASA's counterpart of peer-reviewed formal professional papers but has less stringent limitations on manuscript length and extent of graphic presentations.

- TECHNICAL MEMORANDUM. Scientific and technical findings that are preliminary or of specialized interest, e.g., quick release reports, working papers, and bibliographies that contain minimal annotation. Does not contain extensive analysis.

- CONTRACTOR REPORT. Scientific and technical findings by NASA-sponsored contractors and grantees.

- CONFERENCE PUBLICATION. Collected papers from scientific and technical conferences, symposia, seminars, or other meetings sponsored or cosponsored by NASA.

- SPECIAL PUBLICATION. Scientific, technical, or historical information from NASA programs, projects, and missions, often concerned with subjects having substantial public interest.

- TECHNICAL TRANSLATION. English-language translations of foreign scientific and technical material pertinent to NASA's mission.

Specialized services that complement the STI Program Office's diverse offerings include creating custom thesauri, building customized data bases, organizing and publishing research results . . . even providing videos.

For more information about the NASA STI Program Office, see the following:

- Access the NASA STI Program Home Page at ***http://www.sti.nasa.gov***

- E-mail your question via the Internet to help@sti.nasa.gov

- Fax your question to the NASA Access Help Desk at 301–621–0134

- Telephone the NASA Access Help Desk at 301–621–0390

- Write to:
  NASA Access Help Desk
  NASA Center for AeroSpace Information
  7121 Standard Drive
  Hanover, MD 21076

NASA/TM—2002-211325

Mechanical Testing of IN718 Lattice Block Structures

David L. Krause and John D. Whittenberger
Glenn Research Center, Cleveland, Ohio

Pete T. Kantzos and Mohan G. Hebsur
Ohio Aerospace Institute, Brook Park, Ohio

Prepared for the
131st Annual Meeting and Exhibition
sponsored by the Minerals, Metals, and Materials Society
Seattle, Washington, February 17–21, 2002

National Aeronautics and
Space Administration

Glenn Research Center

January 2002

Acknowledgments

The authors wish to acknowledge the dedication provided by the NASA UEET program that funded this research, especially the guidance and support provided by Mr. Robert D. Draper, Ms. Catherine L. Peddie, and Dr. Robert J. Shaw of the Glenn Research Center. We also would like to recognize the enthusiasm and commitment provided by Mr. Jonathan Priluck of JAMCORP in advocating and improving lattice block materials, and producing all materials for the test program. Finally, the valuable technical assistance and mechanical skills provided during test development and execution by Mr. Stephen J. Smith of Akima Corporation are gratefully acknowledged.

Available from

NASA Center for Aerospace Information
7121 Standard Drive
Hanover, MD 21076

National Technical Information Service
5285 Port Royal Road
Springfield, VA 22100

Available electronically at http://gltrs.grc.nasa.gov/GLTRS

MECHANICAL TESTING OF IN718 LATTICE BLOCK STRUCTURES

David L. Krause and John D. Whittenberger
National Aeronautics and Space Administration
Glenn Research Center
Cleveland, Ohio 44135

Pete T. Kantzos and Mohan G. Hebsur
Ohio Aerospace Institute
Brook Park, Ohio 44142

Abstract

Lattice block construction produces a flat, structurally rigid panel composed of thin ligaments of material arranged in a three-dimensional triangulated truss-like structure. Low-cost methods of producing cast metallic lattice block panels are now available that greatly expand opportunities for using this unique material system in today's high-performance structures. Additional advances are being made in NASA's Ultra Efficient Engine Technology (UEET) program to extend the lattice block concept to superalloy materials. Advantages offered by this combination include high strength, light weight, high stiffness and elevated temperature capabilities. Recently under UEET, the nickel-based superalloy Inconel 718 (IN718) was investment cast into lattice block panels with great success. To evaluate casting quality and lattice block architecture merit, individual ligaments and structural subelement specimens were extracted from the panels. Tensile tests and structural compression and bending strength tests were performed on these specimens. Fatigue testing was also completed for several bend test specimens. This paper first presents metallurgical and optical microscopy analysis of the castings. This is followed by mechanical test results for the tensile ligament tests and the subelement compression and bending strength tests, as well as for the fatigue tests that were performed. These tests generally showed comparable properties to base IN718 with the same heat treatment, and they underscored the benefits offered by lattice block materials. These benefits might be extended with improved architecture such as face sheets.

Introduction

In 1999 the National Aeronautics and Space Administration created the Ultra Efficient Engine Technology research program at the John H. Glenn Research Center at Lewis Field, Cleveland, Ohio. Its vision is "to develop and hand off revolutionary turbine engine propulsion technologies that will enable future generation vehicles over a wide range of flight speeds." The five-year program includes two top level goals: 1.) develop propulsion technologies to enable increases in efficiency and therefore fuel burn reductions of up to 15%, and 2.) develop combustor technologies (configuration and materials) which will enable reductions in Landing/Takeoff NO_x of 70 % relative to 1996 standards.

The Ultra Efficient Engine Technology program contains seven technology areas, with each area working over the 5-year period to gather and design new technologies that address the two top goals. One of the technology areas seeks innovation and improvements in high temperature engine materials and structures. Superalloy lattice block materials have been proposed in the program for static turbine engine components of a supersonic exhaust nozzle, including possible use in actuated panels, exhaust nozzle flaps, and side panel structures.

Lattice block materials have been developed and patented by JAMCORP (Jonathan Aerospace Materials Corporation) of Wilmington, Massachusetts. JAMCORP's method of fabrication produces three-dimensional structures of various configurations with internal matrices of triangles acting as space frames. The structures look similar to bridge trusses, bar joists, or geodesic domes, except that they are on a meso- or micro-scale. This architecture gives high specific strength and stiffness for most materials. JAMCORP has produced lattice block in a variety of parent materials including steels, aluminums, plastics, rubber, ceramics, and specialty alloys.

In NASA's research program, the strength and lightweight benefits of nickel-based superalloy lattice block are being evaluated for high temperature applications.

IN718 Lattice Block Panels

After considering several metals with good general casting properties, Inconel 718 (IN718) was chosen to demonstrate feasibility in the first superalloy casting trials. Hebsur describes casting and processing details in a paper of this symposium [1]. A rectangular flat panel lattice block configuration was selected that resulted in trimmed integral panels 131 mm wide by 290 mm long and 11 mm in height. Layout of the three-dimensional triangulated space frame produced 14 transverse and 31 longitudinal repeating cells, with one cell through the thickness. Material ligaments averaged 1.6 mm in diameter and were connected at lightly reinforced nodes. A typical panel is illustrated in Figure 1.

This geometry was chosen primarily to facilitate the casting process and not to optimize the structure for carrying loads. The arduous flow path from the peripheral gating through the

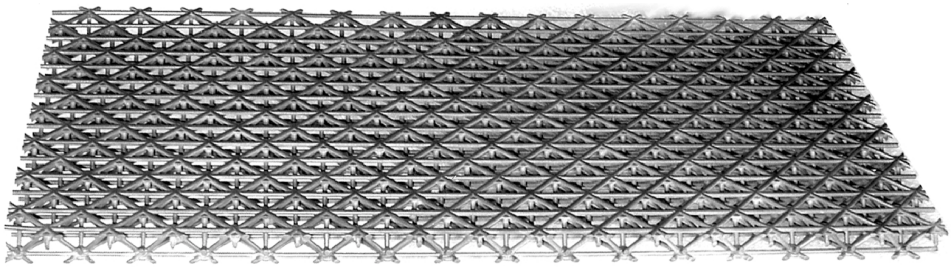

(a)

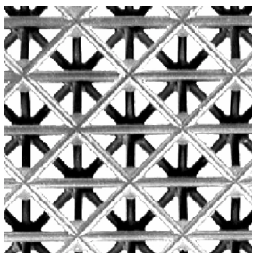

(b)

Figure 1: IN718 lattice block panel 5 after removal of peripheral casting gates; (a) size is 131 mm by 290 mm by 11 mm, (b) enlarged top view shows nodal reinforcement.

tiny ligaments was considered to be the first challenge in demonstrating the technology, with mechanical efficiency to be improved upon later. Simple linear analysis of the panel as configured (Figure 1) showed that specific longitudinal bending stiffness would be 36 % higher than a solid plate; specific bending strength would be 14 % higher.

The superalloy lattice block panels were fabricated by JAMCORP using investment casting in shell molds made from wax patterns. Initially there were numerous problems in making and assembling the wax patterns. During the six-month development program, ten IN718 castings were successfully produced. After careful inspection, the investment casting risers and gates were cut off, and the panels were subjected to a heat treatment as follows: initial hot isostatic pressing (HIP) at 1120 ºC for four hours at 103 MPa in inert argon atmosphere to close internal porosity, followed by one hour at 1010 ºC and an argon gas quench; then eight hours at 718 ºC and a furnace cool to a hold at 620 ºC for at total time at 718/620 ºC of 18 hours.

Panel Physical Characteristics

Overall physical inspection of the ten panels revealed only minor visual defects. Three of the panels were missing one or two ligaments (out of over 2250 per panel) due to lack of fill in the shell molds. Maximum out-of-plane warping seen on the panels was 0.2 to 1.0 mm.

Measuring and weighing eight panels obtained an estimate of the density of the IN718 lattice block. The density values ranged from 1.17 to 1.26 Mg/m^3 with an average of 1.21 Mg/m^3 and a standard deviation of 0.028 Mg/m^3; this average density corresponds to about 15 % of the density of IN718.

Metallurgical examination of unetched, polished, random sections taken from two lattice block panels revealed that the majority of the ligaments were defect free as illustrated in Figure 2a; however a few ligament sections did possess significant amounts of surface connected porosity (Figure 2b) which was not closed by the HIP'ing. Out of a total of 110 ligament cross sections, 85 were whole, 16 had one small casting pore and 9 had multiple (two or more) pores. Figure 2 also illustrates that the ligaments were not cylindrical in cross section, as all possessed "ears" which derived from the split mold used to make the wax pattern for investment casting.

Average diameter, standard deviation and maximum/minimum values were determined from photomicrographs of ligament cross-sections. Two determinations of diameter were made on each 90º section (Figure 2a: perpendicular to the ears and just below the ears) and one measurement of diameter was taken from the diagonal sections (Figure 2b: minor ellipse axis). These diameter values are presented in Table I along with diameters obtained from 166 micrometer measurements of ligaments cut for tensile test specimens. Clearly there are no major discrepancies among the values listed in Table I, which confirms the reproducibility of the investment casting process used for lattice block.

Mechanical Testing Description

Mechanical testing of small portions (ligaments and subelements) of three IN718 lattice block panels has been performed. Samples for testing were electrodischarged machined (EDM'ed) from the panels to provide suitable specimens for ligament tensile and subelement structural testing.

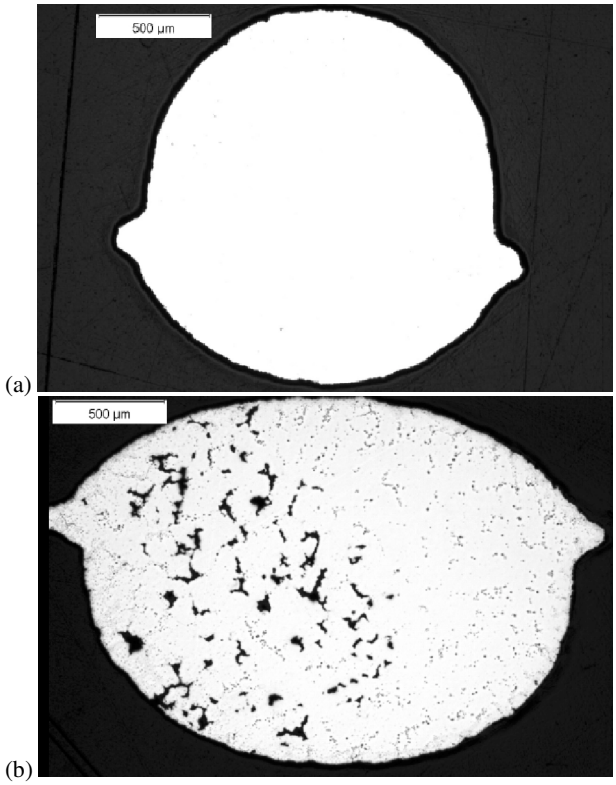

Figure 2: Photomicrographs of unetched, polished IN718 lattice block ligaments from panel 2; (a) 90° cross-section, (b) body diagonal.

Table I Diameter of Ligaments in IN718 Lattice Block

Panel No.	Method	Avg. Diam. (mm)	Std. Dev. (mm)	Max./Min. Diam. (mm)
1	photomicrographs	1.62	0.071	1.76 / 1.52
2	photomicrographs	1.64	0.071	1.80 / 1.54
3	micrometer	1.63	0.045	1.74 / 1.51

Ligament Tensile Testing

Several longitudinal ligaments, approximately 0.3 m in length, were EDM'ed from both the top and bottom faces of one heat-treated IN718 panel for tensile testing of individual ligaments. Each of these lengths was then cut into approximately 0.15 m sections, where one half was reserved for room temperature tensile testing and the other half set aside for 650 ºC testing. Each 0.15 m piece contained eight nodes spaced about 19 mm apart, where the face/body lattice block diagonals intersect the longitudinal ligament. Maximum and minimum diameters were measured for each section between nodes, and all these values were then averaged to give an average diameter for calculation of the cross sectional area of the ligament test specimen assuming an uniform cylindrical geometry. Because the ligaments were not ground to a uniform diameter, the local cross sectional area at each node was much greater than this average diameter.

Tensile testing both at room temperature and at 650 ºC was conducted using a screw driven universal test machine, where the lattice block ligaments samples were gripped at the ends between two nodes using hydraulically controlled, water cooled wedge grips squeezing matched pairs of 9.5 mm diameter by 10 mm long stainless steel inserts with a central 1.5 mm diameter hole. The tensile tests were conducted at a constant velocity to achieve an engineering strain rate of 0.005 per minute in the ligament length between the gripped sections. A probe type extensometer with a 12.7 mm gage was used to measure deformation between the central pair of nodes during both room temperature and 650 ºC testing. A computerized data acquisition system was used to collect load and extensometer data necessary for drawing stress - strain curves for calculation of the offset (0.2%) yield strengths and Ultimate Tensile Strengths (UTS).

Testing at 650 ºC in air was undertaken with a 76 mm tall, one side open, resistance wound, three zone furnace which was centered around the ligament length between the cold grips. Approximately 5 mm thick pieces of pure Ni were inserted in the furnace between the heating elements and test sample to prevent the heating elements from directly shining on the specimen and to smooth the temperature gradients between the three zones. Three thermocouples were used to measure temperature, where the upper and lower thermocouples were tied to the central pair of nodes about 19 mm apart, and the center thermocouple was tied to the midpoint of the

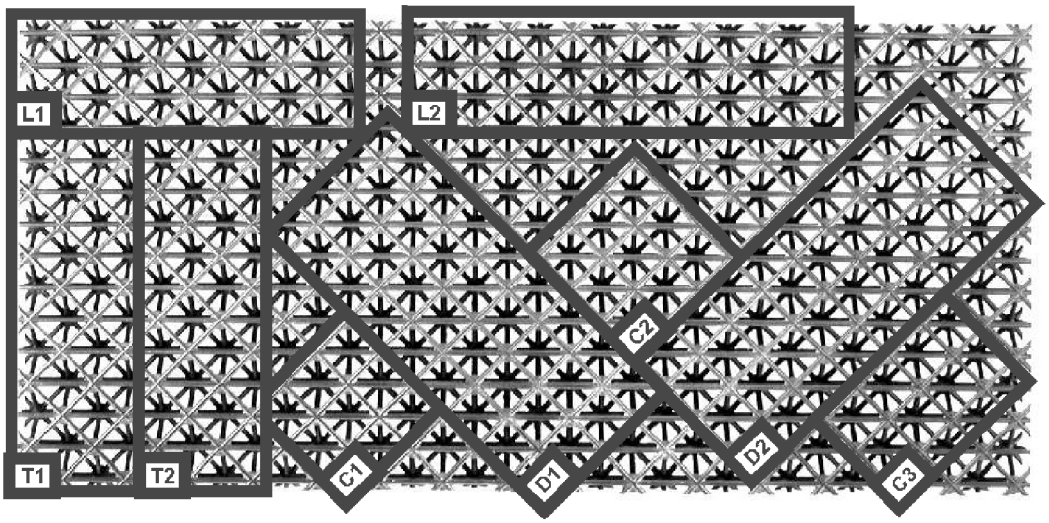

Figure 3: Lattice block panel machining layout and numbering scheme for structural subelement specimens.

ligament section between these two nodes. After gripping the specimen, the furnace was moved into place and the extensometer probes were put into contact with the central reduced section to define the gage length. Both probes were within the length defined by the upper and lower thermocouples.

Once the extensometer was securely in contact with the gage, the open portions of the furnace were carefully packed with insulation to prevent heat loss and chimney effects. Heating the sample to temperature was undertaken under a small stress with the temperature controllers in the manual mode until each thermocouple reached about 640 ºC; at that point in time the furnace controllers were switched to automatic mode. In general the sample was at temperature after about 0.5 h of heating, where the temperature gradient measured ± 4.5 ºC or less. Since the actual length of the heated ligament was not known, all tests were conducted at a crosshead speed of 0.51 mm/minute which corresponds to a engineering strain rate of 0.005 per minute based on the 100 mm separation between grips.

Subelement Structural Testing

Two lattice block panels were machined into smaller subelements for structural compression and bend testing, as indicated in Figure 3. Bend test specimens were oriented to represent the major (longitudinal) and lesser (transverse and diagonal) axes in the face of the panels, with compression test specimens extracted from the remaining areas. Specimen nomenclature is as follows: the first character represents the lattice block panel from which it was cut, the second character defines the specimen's orientation relative to panel direction, and the third character is a sequential number as defined in Figure 3. All subelement testing was performed at room temperature. Because of the difficulty in measuring experimental ligament strains in the subelements, finite element analysis of each configuration was performed to relate experimental loads to ligament stresses, and experimental deflections to ligament strains. The linear elastic analyses were performed using beam elements for ligaments, with no additional reinforcement modeled at nodes; all ligament connections were assumed to be fully moment-carrying. Boundary conditions reflected the actual test conditions of rigid rollers for load application and reaction. Ligament diameters were defined as the average 1.6 mm diameter, and node spacing was set at the average measured panel values: 18.72 mm longitudinally, 9.38 mm transversely, and 9.39 mm through the thickness. The material modulus was set at 191 GPa, and Poisson's ratio was defined as 0.29, based on reported data in the Aerospace Structural Metals Handbook [2].

The subelement structural testing was performed using a hydraulic test machine with all-digital controls. A hydraulically actuated wedge grip was outfitted with a universal joint fixture that permitted axial vertical load to be transmitted, but the joint released rotational degrees of freedom in the horizontal plane (see Figure 4). Total applied force was measured with a calibrated load cell on the hydraulic cylinder; deflections were measured with both the system's linear variable differential transformer and a dial indicator with 0.0254 mm resolution. Rigid top and bottom platens were used to sandwich specimen 1C1 for the one subelement compression strength test performed. For subelement bend tests, a combination of 8 mm and 32 mm solid stainless steel rollers were used with fixtures to apply loads and support the specimens. Four-point bending strength and fatigue tests were completed for specimens 1L1, 1T1, 2L1, and 2T1; three-point bending strength and fatigue tests were done for specimens 1D1 and 2D1 due to the odd number of engaged nodes on the top face.

All strength testing was performed in displacement control, with data being recorded at 0.025 mm increments in the linear behavior range, and generally five to ten times that step size in the plastic region. Tests were terminated when little

significant strength remained after fracture of multiple ligaments, or when the limits of the test fixture were reached.

Fatigue tests were run under load control due to the unavailability of load fixtures for fully reversed cyclic loading. Sinusoidal waveforms were applied at one to two Hertz, with a load ratio (minimum load divided by maximum load) of approximately 10 percent. The first test performed (specimen 2D1) was subjected to an initial stress range of 20 % of its ultimate strength based on the prior strength test of specimen 1D1, followed by stress range increases to 40 % and then 50 % of ultimate strength. The other two fatigue tests (2L1 and 2T1) were cycled at a stress range of 40 % of their expected ultimate strength. Fatigue testing was terminated when multiple ligament fractures significantly reduced subelement stiffness.

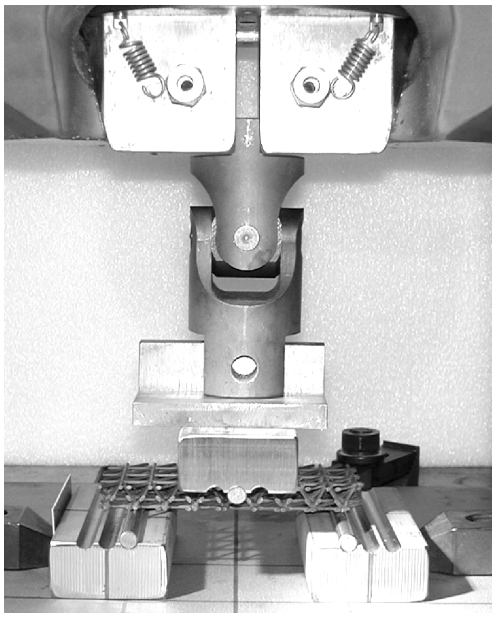

Figure 4: Experimental setup for subelement bend strength testing (specimen 1D1 shown).

Experimental Results

Ligament tensile testing and subelement structural testing produced somewhat different results. In general, the ligament tests revealed lower yield and ultimate strengths and little elongation, while the subelement tests showed high strengths and elongations.

Ligament Tensile Test Results

The average tensile properties measured at room temperature and 650 ºC for individual IN718 lattice block ligaments are given in Table II. Five tests were initially conducted at room temperature with 100 mm long ligament test sections; four of these tests failed prematurely during the elastic deformation, while the fifth test only reached 0.08 % plastic strain before failure. Seven of the broken pieces were retested, because they had undergone only room temperature elastic deformation and were of sufficient length for gripping and the use of the extensometer between a pair of nodes. These retested samples had test section lengths between 29 to 70 mm, and all specimens deformed plastically at room temperature with the total strain at failure ranging from 1.3 to 8.9%. Therefore a size effect appears to exist, where longer lengths of ligament will contain a serious casting defect (Figure 2b), but shorter lengths do not. Figure 5 depicts experimental stress-strain data for three of the shorter specimens.

Based on the room temperature experience with 100 mm long test sections, it was expected that few, if any, of the six 650 ºC tests would demonstrate yielding before failing. However four specimens did plastically deform beyond the proportional limit, but only one sample experienced sufficient deformation for calculation of the 0.2% yield strength (Table II).

Examination of the literature values for the tensile strength of investment cast IN718 indicates that these properties are strongly dependent on processing and the specific heat treatment, where, for example, the Aerospace Structural Metals Handbook [2] reports room temperature yield strengths from 585 to 1000 MPa. Minimum room temperature strength and ductility properties (Table II) are given in [2] for investment cast IN718 which was annealed at 1093 ºC, air-cooled and aged at 720 ºC for 8 hours, then furnace-cooled to 620 ºC and held for a total of age of 18 hours.

Comparison of these minimums to the values obtained for the ductile ligaments indicates that the investment cast lattice block can have tensile properties close to the acceptable range.

Bouse and Behrendt [3] have reported room temperature and 650 ºC tensile results for conventionally cast and HIP'ed (at 1120 ºC) IN718, and these values are also reported in Table II. While the 0.2% yield strength properties for the IN718 lattice block ligaments compare favorably with the conventionally cast/HIP IN718 at both temperatures, neither the ultimate tensile strengths nor tensile elongations do. Presumably the low tensile ductilities found in the IN718 ligaments are due to casting defects like that seen in Figure 2b, which localize deformation to a smaller volume with a reduced load bearing area. This, in turn, lowers the calculated ligament ultimate tensile strength because of the lesser load required to fracture a diminished cross section.

Table II Tensile Properties of IN718 Ligaments

Test Temp. (°C)	Gage Length (mm)	0.2% Yield Strength (MPa) Avg./Std. Dev.	Ult. Tensile Strength (MPa) Avg./Std. Dev.	Elongation (%) Avg./Std. Dev.
RT	100	- / -	627[1]/ 150	- / -
RT	29-70	757 / 24	827 / 32	4.3 / 2.9
650	100	630[2]/ -	582[1]/ 111	- / -
RT[3]		760	860	5
RT[4]		830	970	16
650[4]		650	720	16

[1]Fracture stress
[2]Single value
[3]See reference [2]
[4]See reference [3]

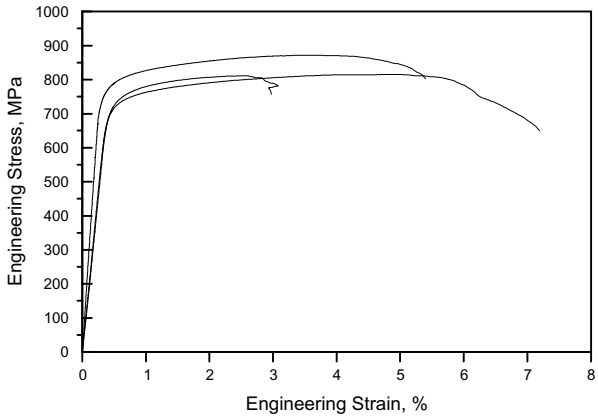

Figure 5: Representative stress-strain diagrams from room temperature testing of 29 to 70 mm lengths of IN718 ligament.

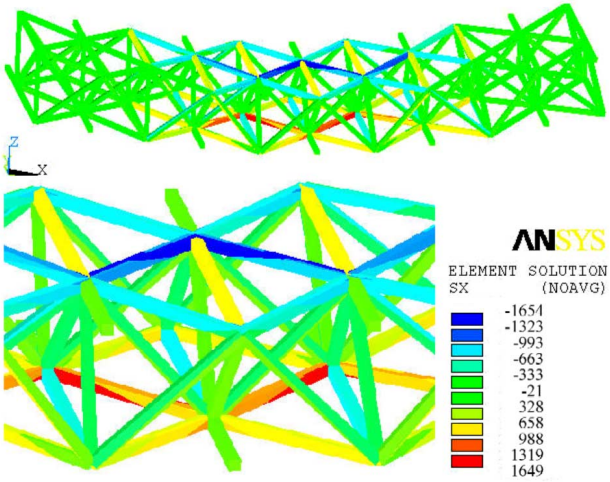

Figure 6: Representative finite element analysis; ligament longitudinal stresses (MPa) for specimen 1T1 with 2.60 kN load applied.

Subelement Structural Test Results

As previously described, beam-element finite element analysis of each specimen configuration was performed to relate loads, ligament stresses, and ligament strains (Figure 6, for example). Maximum and minimum ligament stresses reported here were determined by multiplying the measured experimental loads by an appropriate analytically determined factor; likewise, ligament strains were derived by multiplying experimental deflections by the appropriate factor. Because the analyses were linear elastic, they did not predict the inelastic buckling phenomena of compression ligaments nor second order effects that occurred in most of the strength tests. The consequence of using the linear analyses' factors on the experimental data beyond the yield point is many-fold; two effects are noted here. First, calculated maximum stresses for some compressive ligaments are under-reported, as buckled members released load that was redistributed to other compression members to maintain equilibrium. And secondly, local strains for buckled ligaments are grossly under-reported (buckled member curvature radii as small as three times the ligament diameter were common), while tension ligament strains are over-reported due to the decreased specimen stiffness.

The plots and data that follow are not modified to account for these plastic deformation effects. However, the general conclusions reached are little affected, since structural failure of the lattice block subelements for bend tests was defined by the tensile fracture of tension ligaments, not by loss of stiffness due to compressive ligament buckling. For the fatigue tests, load application remained in the elastic range and consideration of buckling does not apply. Only the compression strength test results are much affected, but since this type of loading is not an efficient use of the lattice block architecture, and since this loading is not applicable to any of the proposed uses for lattice block, it has not been analyzed further.

Compression Strength Test Results Specimen 1C1 was a four-cell lattice block subelement. The top face grid of ligaments was located one-half cell longitudinally and one-half cell transversely from the bottom face grid. This arrangement produced a net lateral force on the structure when subjected to a vertical, through-thickness pressure load. The result was that some of the ligaments were loaded in tension, even though the global loading was compressive. Upon loading, specimen 1C1 exhibited initial stiffening thought to be fixture-related. This was followed by nearly linear response up to a maximum load of 24.0 kN. The specimen deformed plastically after this point to a thickness compression of 1.87 mm, roughly 20 % of its total thickness, where the test was terminated with no ligament fractures apparent. Approximately one-half of the diagonal ligaments in the thickness direction were buckled. The calculated peak compressive stress of 1060 MPa occurred at 0.59 % strain; the peak tensile stress of 570 MPa occurred at 0.32 % strain. Ligament strains at test termination were 1.92 % in compression and 1.03 % in tension. Figure 7 shows the stress-strain diagram for the compression strength test.

The analysis predicted much higher stiffness than that observed. For the linear portion of the test (up to 20 kN load), experimental deflections were 2.44 times the analytical prediction. This may be related to early buckling of compression ligaments or not developing full ligament end moments at nodes.

Bending Strength Test Results One bending strength test was performed for subelements in each of the three lattice block panel strength axes. The calculated stress-strain diagrams for the three tests are shown in Figure 8. As expected, the four-point loaded longitudinally oriented specimen 1L1 carried the largest maximum load due to its advantageous arrangement

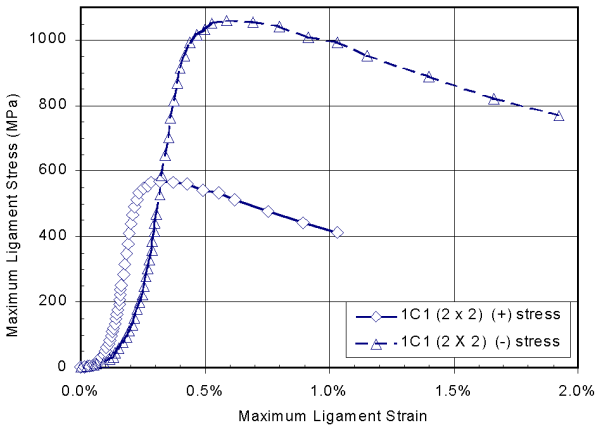

Figure 7: Stress-strain diagram for compression strength test of specimen 1C1.

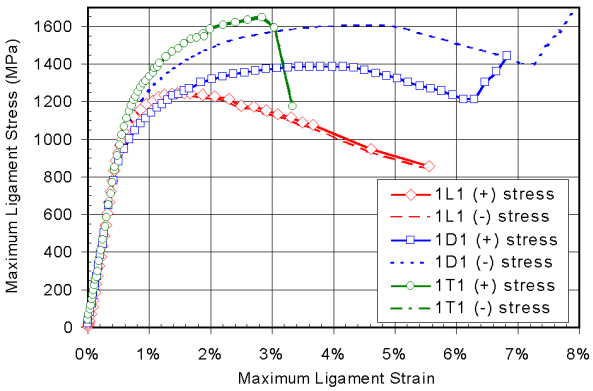

Figure 8: Stress-strain diagrams for three lattice block subelement strength tests.

of ligaments. Linear behavior was evident until approximately 5.00 kN and 0.73 mm; at this load the analysis predicted 0.66 mm total deflection, about 9 % stiffer than experimentally measured. The smaller deflections predicted by the finite element analyses might be due to the boundary conditions imposed. The analysis assumed vertical supports at the end nodes of all four longitudinal ligament rows. But because of the deflected shape, two of the outer-most nodes on each end of the specimen actually lifted off of the support roller, an effect not modeled that would allow greater deflections.

The peak load carried by specimen 1L1 was 6.37 kN, and the test ended at the maximum deflection of 7.53 mm, when the fixture limits were reached. The maximum deflection-to-span ratio was 1/9.94. One ligament was believed to have fractured based on audible detection soon after peak load was reached, although the fracture could not be visually observed. The center eighteen cells of top longitudinal and diagonal ligaments were highly buckled, along with most compression vertical diagonals in this area. The buckled ligaments are readily visible in Figure 9. The calculated peak ligament stresses of 1250 MPa in tension and 1230 MPa in compression occurred at 1.56 % strain. Strains at test termination were 5.55 % in tension and 5.48 % in compression.

Figure 9: Post-test photographs of specimen 1L1 showing buckled compression ligaments; (a) top view, (b) side view.

Specimen 1D1 was the diagonally oriented specimen and was a three-point bend test because of node alignment. It carried a moderate load due to its longitudinal arrangement of face diagonal ligaments. Linear behavior was exhibited until approximately 2.50 kN and 0.65 mm; at this load the analysis predicted 0.72 mm total deflection, about 12 % less stiff than experimentally measured. The smaller experimental deflections might be due to the extra material reinforcing the ligaments at the connecting nodes. The analysis did not model this extra stiffness.

Beyond this linear range, a broad deflection curve for specimen 1D1 gradually peaked at a maximum load of 4.20 kN, and the test ended at the fixture-limited maximum deflection of 9.73 mm. The deflection-to-span ratio at this point was 1/9.54. No ligaments were believed to have fractured based on experimental observation. The specimen was oriented with two cells across the width on the top face and three across the bottom face. This asymmetrical cross-section about the horizontal neutral axis led to higher stresses and strains in the top face ligaments than in the bottom face ligaments. The center four cells of top longitudinal and diagonal ligaments were highly buckled at the end of the test, with only minor buckling of the vertical diagonals in this area. The calculated peak tensile ligament stress was 1390 MPa at 3.80 % strain; the calculated peak compressive stress was 1600 MPa at 4.39 % strain. Strains at test termination were 6.83 % in tension and 7.89 % in compression.

The final bending strength test was the four-point loaded transversely oriented specimen 1T1, which carried the smallest maximum load due to its lack of longitudinally oriented face ligaments. The subelement behaved linearly until approximately 1.70 kN and 0.84 mm; at this load the analysis predicted 1.07 mm total deflection, which was 28 % less stiff than experimentally measured. The extra specimen stiffness might be due to the unmodeled nodal reinforcement. This effect would be particularly large for specimen 1T1, as all extreme fiber stress was transmitted in a zigzag fashion in the top and bottom face ligaments through the effectively reinforced nodes. This would be somewhat offset by the

increased flexibility due to lift-off from the outer roller supports as described earlier for specimen 1L1.

The peak load carried by specimen 1T1 was 2.60 kN, and this was quickly followed by test termination at the maximum deflection of 4.65 mm, when multiple tension ligaments fractured. The deflection-to-span ratio at failure was 1/16.1. Ligament breaks were not detected prior to the final stroke step, and ligament buckling also was not observed. The calculated peak ligament stress of 1650 MPa in tension and compression occurred at 2.84 % strain. The actual stresses were likely lower, again due to the presence of the nodal reinforcement material. A maximum strain 3.34 % was reached just prior to failure.

Bending Fatigue Test Results All three specimens were tested until complete failure of tension ligaments in the area of maximum moment. Cracks propagated through the longitudinal and diagonal bottom face ligaments in the center cells, as well as in the vertical through-thickness tension ligaments. Specimen deflections increased in steps throughout the load-controlled test duration, presumably increasing as individual ligaments failed.

Specimen 2D1 survived for 240,000 cycles at a minimum-to-maximum load range of 0.845 kN and for 247,000 cycles at 1.69 kN with no discernable breaks. The test was completed after an additional 160,000 cycles at 2.14 kN. Following this test, specimen 2L1 was fatigue tested under a load range of 2.55 kN, and it failed after 87,800 cycles. Finally, specimen 2T1 was tested under a load range of 1.04 kN, and it failed after 637,000 cycles.

Because fatigue life curves were not available in the literature for cast IN718 with the particular heat treatment described earlier, empirical curves were generated based on the material's physical properties. Manson's Method of Universal Slopes [4] was used to establish the base curve for fully reversed straining using the following relationship:

$$\Delta\varepsilon_{total} = 3.5\,(\sigma_{UTS}/E)\,(N_{fo})^{-0.12} + D^{0.6}\,(N_{fo})^{-0.6} \quad (1)$$

where
$\Delta\varepsilon_{total}$ = total alternating strain range
σ_{UTS} = ultimate tensile strength
E = modulus of elasticity
N_{fo} = cycles to failure for fully reversed straining
D = true ductility = ln (100/(100-RA)]
RA = reduction of area in tensile test, %

Base curves were established for each specimen using the experimental σ_{UTS} values from the earlier bending strength tests and using the Aerospace Structural Metals Handbook [2] values for E of 191 GPa and for RA of 37 %.

These base curves were then modified for the presence of a non-zero mean strain, since as stated previously the load ratio was 10 %. The Halford–Modified Morrow Mean Stress Model [5] was employed using the following equation:

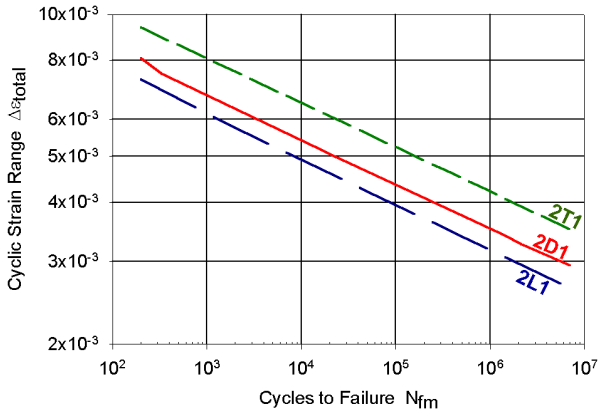

Figure 10: Empirical life prediction curves for cast IN718 lattice block material, adjusted for load ratio R = 0.10.

$$(N_{fm})^{-b} = (N_{fo})^{-b} - V_{\sigma} \quad (2)$$

where
N_{fm} = cycles to failure with applied mean stress
N_{fo} = cycles to failure for fully reversed straining
b = slope of elastic line (assumed equal to 0.1)
V_{σ} = ratio of mean stress to alternating stress

The modified cycles to failure were used to shift the three fatigue life curves to account for the 10 % load ratio, and the final curves are shown in Figure 10.

The variable specimen maximum deflections under constant cyclic load applications required manipulation of the data to compare to the strain-life cycles fatigue curves. The deflection records were grouped into smaller clusters with similar deflection ranges, and constant strain ranges were calculated for these clusters. The strains were determined using the same factors that were used in the bending strength test calculations. This method results in calculated strains lower than actually present due to increased strains upon progressive fracture of nearby ligaments. A final modification to the experimental strains was made to account for the geometric discontinuity at the ligament-node joint. A fatigue strain intensification factor of 1.50 was applied as a reasonable approximation. The cumulative fatigue damage for these strain clusters was then calculated using the Damage Curve Approach of Manson and Halford [6]:

$$n_{i+1}/N_{i+1} = 1 - (n_i/N_i)^{(N_i/N_{i+1})^{0.4}} \quad (3)$$

where
n_i = number of applied cycles at strain range i
n_{i+1} = number of available cycles at strain range i+1
N_i = total calculated cycles to failure for strain range i
N_{i+1} = total calculated cycles to failure for strain range i+1

Results of these calculations are summarized in Table III. As can be seen, specimens 2D1 and 2L1 exceeded the predictions; however, these data points are realistically within the margin of uncertainty for the empirical-derived fatigue life prediction. Specimen 2T1 fell far short of the forecast, which was for approximately infinite life. One possible cause was the high ultimate strength assumption (1650 GPa), which greatly influenced the life prediction. Another reason may be related to the unusual behavior of the specimen. Under constant cyclic load (i.e. stress) range, the deflections *decreased* by the end of the test to only 65 % of their initial values. This unexplained behavior resulted in low experimental strains and the accompanying long predicted fatigue life.

Table III Bending Fatigue Tests Analyses

	Specimen ID		
	2D1	2L1	2T1
Strain Range[1] 1 $\Delta\varepsilon_{total}$	0.16%	0.34%	0.46%
Predicted # Cycles[2] N_1	~ ∞	538000	361000
Experimental Cycles n_1	241000	53360	77100
Available Cycles at S.R. 2	212000	175000	10100000
Strain Range[1] 2 $\Delta\varepsilon_{total}$	0.33%	0.37%	0.29%
Predicted # Cycles[2] N_2	2120000	180000	~ ∞
Experimental Cycles n_2	247000	9840	293400
Available Cycles at S.R. 3	246000	56100	6220000
Strain Range[1] 3 $\Delta\varepsilon_{total}$	0.40%	0.42%	0.30%
Predicted # Cycles[2] N_3	248000	58300	~ ∞
Experimental Cycles n_3	100000	19680	266831
Available Cycles at S.R. 4	17200	2370	failed
Strain Range[1] 4 $\Delta\varepsilon_{total}$	0.51%	0.56%	
Predicted # Cycles[2] N_4	18800	2520	
Experimental Cycles n_4	56000	4880	
Available Cycles at S.R. 5	---	failed	
Strain Range[1] 5 $\Delta\varepsilon_{total}$	0.75%		
Predicted # Cycles[2] N_5	334		
Experimental Cycles n_5	4395		
Available Cycles at S.R. 6	failed		

[1]Range includes strain concentration factor of 1.5

[2]Prediction is based on load ratio = 0.10

Future Plans

More detailed finite element analyses of the subelements are planned, using solid elements to model the ligaments, nodes, and nodal reinforcements. This could result in improved understanding of lattice block behavior and the significance and design of its features, especially the reinforcements.

Another series of subelement structural tests of IN718 specimens is planned for 650 ºC that will duplicate most of the room temperature tests performed. In addition, full panels will be tested with pseudo-pressure loadings at room temperature and 650 ºC. Possible future tests also include testing of lattice block subelements with either one or two integral IN718 face sheets. Preliminary estimates show that large gains can be made in specific strength and stiffness over the open-faced lattice block architecture for bending elements.

Finally, experimental investigation is planned for higher-temperature alloys. MarM247 has been successfully cast as lattice block and will be tested in the same manner as IN718.

Concluding Remarks

Porosity or other casting defects likely caused size effect premature failures and low ductilities in ligament tensile testing. Of course poor ligament properties in areas of highest stress would reduce the quality of components fabricated from lattice block material. For this reason the early IN718 lattice block casting practice has to be improved.

Compression strength testing was the first subelement test performed and gave surprising results. Unexpected inelastic buckling of compression ligaments enabled large structural deflection. This phenomenon could be advantageous for some applications and not for others. Revising the lattice block geometry or ligament cross-section could promote or lessen the occurrence. Casting defects have little effect on compressive strength.

For structural elements carrying mainly bending loads, strength testing of bend specimens showed that lattice block architecture has several important benefits besides inherent light weight and high stiffness. These include: damage-tolerant design, evident by the continued strength even with fractured and buckled ligaments; large, readily-observable deflections prior to breaking; and, load spreading ability due to many load path redundancies. For structures in bending, only a fraction of the loaded material is at the highest stress level; for this reason, reduced strength related to the size effect was not observed. The bending strength tests were generally limited by the base material ultimate tensile strength, rather than the structure of the lattice.

In fatigue-limited designs, lattice block has advantages similar to static bending, primarily that significant life remains after failure of initial ligaments. However, for fatigue loading in the elastic range, ligament failure may not be observable by plastic distortion, and the disadvantage of difficult nondestructive examination of the lattice ligaments becomes important.

Summary

Superalloy lattice block materials are being investigated for aero-propulsion uses; successful lattice block panels have been investment cast in Inconel 718 superalloy. Following inspection, these panels were cut into smaller specimens for mechanical testing of physical properties. The testing included ligament tensile tests and subelement compression, bending strength, and bending fatigue tests. The subelement tests generally resulted in material properties equal with IN718 base properties, but higher than detected by the tensile

tests. This might be due to the presence of casting defects and a size effect. The promising preliminary results hint at beneficial use for a variety of applications, and have led to plans for additional testing with IN718 as well as higher temperature aerospace alloys.

References

1. M. Hebsur, "Processing of IN-718 Lattice Block Castings," (Paper presented at the TMS Third Global Symposium, Processing and Properties of Lightweight Cellular Metals and Structures, Seattle, Washington, 17–21 February 2002).

2. W.F. Brown Jr., H. Mindlin, C.Y. Ho, eds., Aerospace Structural Metals Handbook, vol. 4 (West Lafayette, IN: CINDAS/USAF CRDA Handbooks Operation, Purdue University, 1996), Code 4103.

3. G.K Bouse and M.R. Behrendt, "Superalloy 718 - Metallurgy and Applications," ed. E.A. Loria (Warrendale, PA: The Minerals, Metals & Materials Society, 1989), 319–328.

4. S.S. Manson, "Fatigue – A Complex Subject," Experimental Mechanics, 5 (7) (1965), 193–226.

5. G.R. Halford and A.J. Nachtigall, "The Strainrange Partitioning Behavior of an Advanced Gas Turbine Disk Alloy, AF2-1DA," J. Aircraft, 17 (8) (1980), 598–604.

6. S.S. Manson and G.R. Halford, "Practical Implementation of the Double Linear Damage Rule and Damage Curve Approach for Treating Cumulative Fatigue Damage," International Journal of Fracture, 17 (1981), 169–192.

REPORT DOCUMENTATION PAGE

Form Approved
OMB No. 0704-0188

Public reporting burden for this collection of information is estimated to average 1 hour per response, including the time for reviewing instructions, searching existing data sources, gathering and maintaining the data needed, and completing and reviewing the collection of information. Send comments regarding this burden estimate or any other aspect of this collection of information, including suggestions for reducing this burden, to Washington Headquarters Services, Directorate for Information Operations and Reports, 1215 Jefferson Davis Highway, Suite 1204, Arlington, VA 22202-4302, and to the Office of Management and Budget, Paperwork Reduction Project (0704-0188), Washington, DC 20503.

1. AGENCY USE ONLY (*Leave blank*)

2. REPORT DATE
January 2002

3. REPORT TYPE AND DATES COVERED
Technical Memorandum

4. TITLE AND SUBTITLE
Mechanical Testing of IN718 Lattice Block Structures

5. FUNDING NUMBERS
WU–714–04–50–00

6. AUTHOR(S)
David L. Krause, John D. Whittenberger, Pete T. Kantzos, and Mohan G. Hebsur

7. PERFORMING ORGANIZATION NAME(S) AND ADDRESS(ES)
National Aeronautics and Space Administration
John H. Glenn Research Center at Lewis Field
Cleveland, Ohio 44135–3191

8. PERFORMING ORGANIZATION REPORT NUMBER
E–13124

9. SPONSORING/MONITORING AGENCY NAME(S) AND ADDRESS(ES)
National Aeronautics and Space Administration
Washington, DC 20546–0001

10. SPONSORING/MONITORING AGENCY REPORT NUMBER
NASA TM—2002-211325

11. SUPPLEMENTARY NOTES
Prepared for the 131st Annual Meeting and Exhibition sponsored by the Minerals, Metals, and Materials Society Seattle, Washington, February 17–21, 2002. David L. Krause and John D. Whittenberger, NASA Glenn Research Center; Pete T. Kantzos and Mohan G. Hebsur, Ohio Aerospace Institute, 22800 Cedar Point Road, Brook Park, Ohio 44142. Responsible person, David L. Krause, organization code 5920, 216–433–5465.

12a. DISTRIBUTION/AVAILABILITY STATEMENT
Unclassified - Unlimited
Subject Category: 26 Distribution: Nonstandard
Available electronically at http://gltrs.grc.nasa.gov/GLTRS
This publication is available from the NASA Center for AeroSpace Information, 301–621–0390.

12b. DISTRIBUTION CODE

13. ABSTRACT ***(Maximum 200 words)***

Lattice block construction produces a flat, structurally rigid panel composed of thin ligaments of material arranged in a three-dimensional triangulated truss-like structure. Low-cost methods of producing cast metallic lattice block panels are now available that greatly expand opportunities for using this unique material system in today's high-performance structures. Additional advances are being made in NASA's Ultra Efficient Engine Technology (UEET) program to extend the lattice block concept to superalloy materials. Advantages offered by this combination include high strength, light weight, high stiffness and elevated temperature capabilities. Recently under UEET, the nickel-based superalloy Inconel 718 (IN718) was investment cast into lattice block panels with great success. To evaluate casting quality and lattice block architecture merit, individual ligaments, and structural subelement specimens were extracted from the panels. Tensile tests, structural compression, and bending strength tests were performed on these specimens. Fatigue testing was also completed for several bend test specimens. This paper first presents metallurgical and optical microscopy analysis of the castings. This is followed by mechanical test results for the tensile ligament tests and the subelement compression and bending strength tests, as well as for the fatigue tests that were performed. These tests generally showed comparable properties to base IN718 with the same heat treatment, and they underscored the benefits offered by lattice block materials. These benefits might be extended with improved architecture such as face sheets.

14. SUBJECT TERMS
Structures; Trusses; Cells; Investment casting; Inconel; Mechanical properties; Deformation; Tensile strength; Modulus of elasticity; Compressive strength; Bending; Flexural strength; Fatigue life

15. NUMBER OF PAGES
16

16. PRICE CODE

17. SECURITY CLASSIFICATION OF REPORT
Unclassified

18. SECURITY CLASSIFICATION OF THIS PAGE
Unclassified

19. SECURITY CLASSIFICATION OF ABSTRACT
Unclassified

20. LIMITATION OF ABSTRACT